SAND2008-3130P

Application of a Low-Dissipation Finite Volume Scheme to a Blunt-Body Re-entry Flow

To appear in: H.C. Yee, *High order numerical schemes for hypersonic flow simulations*, Von Karman Institute Lecture Series : "Course on Hypersonic Entry and Cruise Vehicles"

Matthew Barone
Sandia National Laboratories*
MS 0825, P.O. Box 5800 Albuquerque, NM 87185-0825

May 9, 2008

Low-dissipation, Locally Positive, Finite Volume Scheme

Rather than implementing the low-dissipation scheme using a filter numerical flux, the flow sensor can be incorporated directly into the definition of a numerical flux. This approach does not take full advantage of the accuracy and efficiency of the filter approach; however, it may allow for improved stability of the scheme and preservation of positivity in the presence of discontinuous flow features.

A scheme that incorporates the flow sensor into the numerical flux definition has been recently developed. The details of the scheme are derived in [1], with only the essential elements given here. There are two parts to constructing the scheme. The basic idea for the first part is to use the framework provided by Jameson [2] to extend a second order positive scheme to fourth order, while maintaining positivity. This is accomplished by addition of a corrective flux to a baseline second order flux. The baseline flux that is used is the second order Symmetric Limited Positive (SLIP) scheme [2], which is essentially identical to the Symmetric TVD scheme [3]. The fourth order SLIP scheme is thus written,

$$\mathbf{F}^{SLIP4}_{j+1/2} = \mathbf{F}^{SLIP2}_{j+1/2} + \mathbf{F}^{C}_{j+1/2}. \tag{1}$$

The corrective flux includes corrections to both the centered difference and the dissipative parts of the lower order flux. It is only added if it locally satisfies a bound that ensures that the scheme remains Local Extremum Diminishing (LED).

The second part of the scheme involves incorporating a flow sensor to reduce the numerical dissipation in regions of smooth flow. This is done by multiplying both the low order dissipation term and the dissipative component of the corrective flux by the flow sensor

*Sandia is a multiprogram laboratory operated by Sandia Corporation, a Lockheed Martin Company for the United States Department of Energy's National Nuclear Security Administration under contract DE-AC04-94AL85000

in characteristic variable space. Best results have been obtained using the wavelet-based flow sensor described in [4]. More specifically, the redundant wavelet from Harten's multi-resolution method, or "RH-wavelet" sensor, is used. Three levels of wavelet coefficients are employed on each block of a multiblock structured mesh. There is some freedom in specifying the function relating the value of the sensor, $\theta^l_{j+1/2}$, to the measure of solution regularity, or Lipschitz exponent α. This is the function $\tau(\alpha)$ in the notation of Ref. [4]. We use the simple function

$$\theta^l_{j+1/2} = \tau(\alpha^l_{j+1/2}) = \begin{cases} 1, & \alpha \leq 0.5 \\ \frac{1-\alpha}{1-\alpha_0}, & 0.5 < \alpha < 1.0 \\ 0, & \alpha \geq 1.0 \end{cases} \tag{2}$$

Note that the LED property of the base flux scheme is preserved when $\theta^l_{j+1/2} = 1$. Also note that the resulting scheme is only fourth order for a scalar equation on a uniform mesh, and is formally second order accurate otherwise. Despite this, the error on a given mesh level for unsteady compressible flow applications is substantially lower for the low-dissipation scheme than for the standard second order SLIP scheme [1].

The last implementation detail is the treatment at non-periodic domain boundaries. Here, the cell-centered characteristic variables are reflected across the domain boundary, allowing the full wavelet stencil to be populated at the near-boundary cells. This is done both at physical domain boundaries and inter-block boundaries. However, at the boundary interface ($j = 1/2$ and $j = N + 1/2$), a modified form of the ACM fow sensor [5] is applied, giving a consistent flux across inter-block boundaries.

Example: Unsteady Simulation of Space Capsule Re-entry

The low-dissipation scheme was used to simulate the flow of air past the NASA Orion Command Module (CM) for two supersonic flow conditions. The first condition corresponds to supersonic flight at Mach number of 2.5 and angle of attack of 142 degrees (measured from the pilot-forward axis). The Reynolds number based on the maximum vehicle diameter for this case is $Re_D = 5.30 \times 10^6$. Adiabatic wall boundary conditions were applied. The second condition is flow at Mach 16, $Re_D = 1.76 \times 10^6$, and angle of attack of 180 degrees at an altitude of 35 km, corresponding very closely to the Fire II vehicle conditions that were simulated in Ref. [6]. A constant wall temperature of 553.3 K is prescribed. An ideal gas equation of state, along with Sutherland's law for viscosity and a constant Prandtl number assumption, were used in both simulations. This obviously results in an inadequate physical description of the gas for the Mach 16 case. However, the purpose of this exercise is to investigate the robustness of the solution method and the qualitative aspects of the solutions that are generated.

The same grid is used for both cases, and consists of 46 adjoining blocks, with grid cells clustered near the body surface and in the near-wake region. A cross-section of the grid topology is shown in Figure 1. A total of 17.85 million grid cells are used, of which approximately 3.5 million are located in the separated flow/near-wake region. The wall

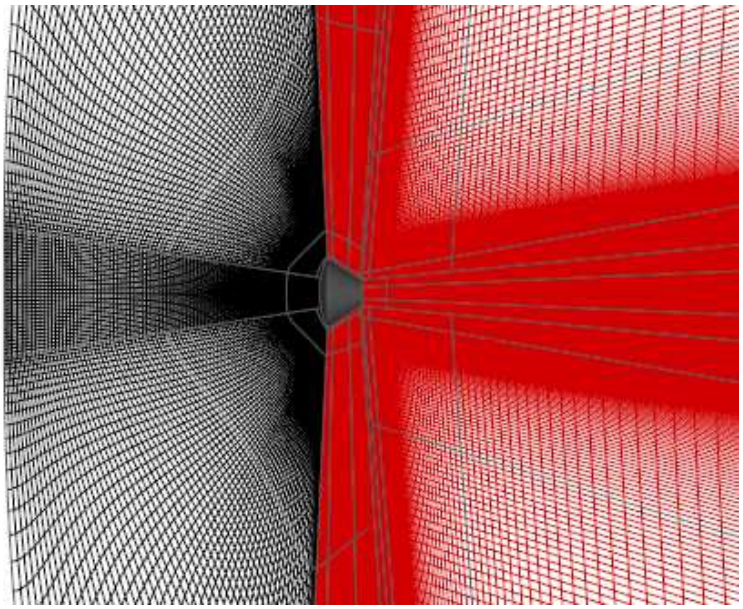

Figure 1: Cut through the computational grid for the Orion CM simulations. For the Mach 16 case, black zones were solved with the first order Roe scheme, red zones with the low-dissipation scheme.

normal cell spacing on the body surface was kept at a nearly uniform value of $\Delta/D \approx 1.0 \times 10^{-5}$. The non-dimensional time step used for the simulation was $\Delta t U_\infty/D = 0.0131$.

The low-dissipation finite volume scheme has been implemented in the Sandia Advanced Code for Compressible Aerothermodynamics Research and Applications (SACCARA), a multi-block, structured grid, compressible Navier-Stokes code [7]. SACCARA allows for different numerical schemes to be applied on different grid blocks. For the Mach 2.5 case, the low-dissipation scheme was applied uniformly over all the grid blocks. For the Mach 16 case, a first order Roe scheme with a relatively high value for the entropy fix was applied for grid blocks forward of, and adjoining with, the Orion forebody. This was to circumvent the carbuncle instability that is a known deficiency of the Roe flux. The low-dissipation scheme was applied everywhere downstream of the forebody region, including the afterbody wake region (see Figure 1). A separate simulation was performed on the same grid, but using the second order SLIP scheme in place of the low-dissipation scheme.

Turbulence was modeled using Detached Eddy Simulation [8], a hybrid model that applies the Spalart-Allmaras one-equation model near solid walls and transitions to an LES subgrid stress model in regions of separated flow away from solid surface. No boundary layer transition model was used, *i.e.* the model was run "fully turbulent."

Figure 2 compares computed time-averaged surface pressure coefficients with experimental values for the Mach 2.5 case. The surface pressures agree well except for some discrepancy near the stagnation point. Figure 3 shows isosurfaces of the "Q" criterion for vortex identification. The wake contains three dimensional vortical disturbances, with finer scale features in the vehicle base region and larger structures oriented in the flow direction shed further up on the afterbody.

For the Mach 16 case, Figure 4 compares instantaneous snapshots of the symmetry plane

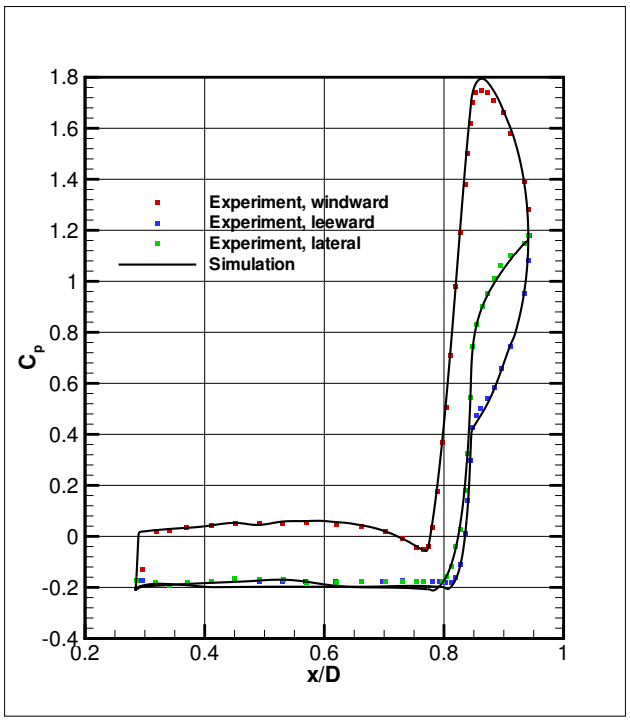

Figure 2: Time-averaged surface pressure coefficient for the $M_\infty = 2.5$ simulation, compared with the experimental data from Ref. [9]. The x coordinate is measured from the vehicle cone apex.

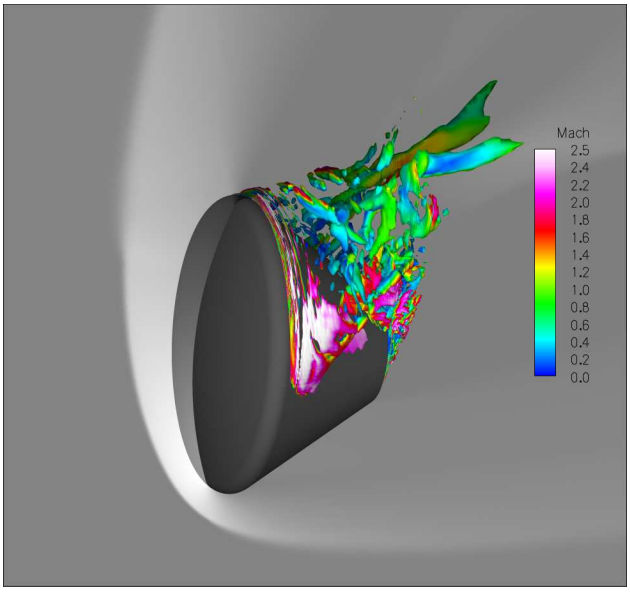

Figure 3: Instantaneous flowfield from the $M_\infty = 2.5$ simulation. Contours of Mach number color an isosurface of $Q \equiv \frac{1}{2}(\Omega_{ij}\Omega ij - S_{ij}S_{ij})$, visualizing vortical structures in the wake. The grayscale contours of pressure indicate the bow shock location.

streamwise vorticity field at identical times for the SLIP2 and low-dissipation simulations. In this flow, as with the lower Mach number case, the bow shock remains essentially steady, with a region of massively separated flow occuring from just aft of the capsule shoulder. Both numerical schemes produce an unsteady, and three-dimensional, wake. However, the low-dissipation scheme produces energetic disturbances at smaller scales, with the more dissipative SLIP2 scheme tending to smear out these small-scale disturbances. Figure 5 compares instantaneous snapshots of the surface heat flux. Essentially the same observation holds true, with the low-dissipation scheme producing smaller-scale features that tend to be diffused by the SLIP2 scheme.

(a) (b)

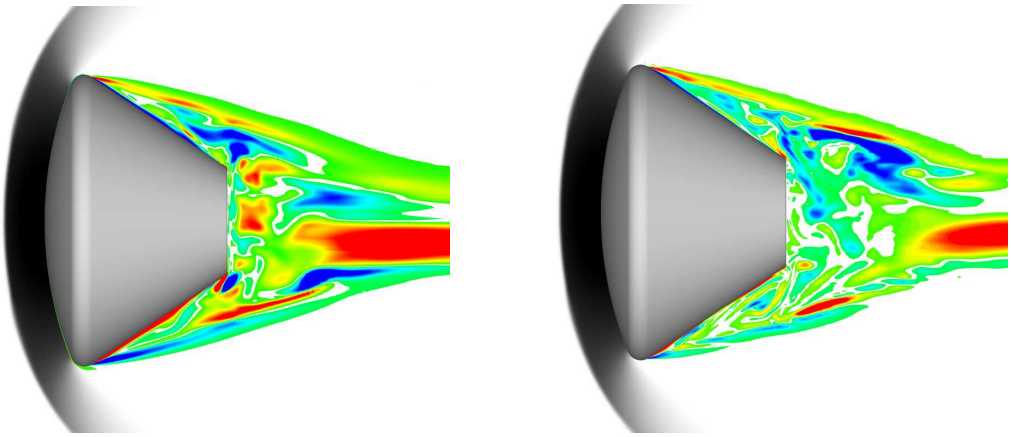

Figure 4: Instantaneous images of the flow on the symmetry plane of the capsule. Grayscale contours are of pressure, showing the location of the bow shock. Color contours are of stream-wise vorticity, Ω_x. (a) Second Order SLIP scheme. (b) Low-dissipation scheme.

(a) (b)

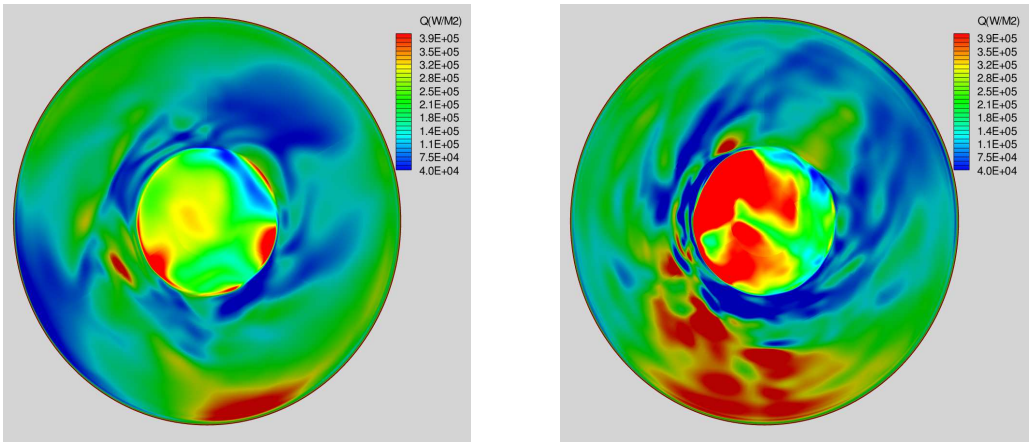

Figure 5: Instantaneous contours of the surface heat flux. (a) Second Order SLIP scheme. (b) Low-dissipation scheme.

References

[1] M.F. Barone. A low-dissipation, locally positive finite volume scheme for compressible flow. in preparation, 2008.

[2] A. Jameson. Analysis and design of numerical schemes for gas dynamics 1: Artificial diffusion, upwind biasing, limiters, and their effect on accuracy and multigrid convergence. *Int. J. Comp. Fluid Dyn.*, 4:171–218, 1995.

[3] H. C. Yee. Implicit and symmetric shock capturing schemes. NASA-TM-89464, May 1987.

[4] B. Sjögreen and H.C. Yee. Multiresolution wavelet based adaptive numerical dissipation control for high order methods. *J. Scientific Computing*, 20(2):211–255, 2004.

[5] H. C. Yee, N. D. Sandham, and M. J. Djomehri. Low-dissipative high-order shock-capturing methods using characteristic-based filters. *J. Comp. Physics*, 150:199–238, 1999.

[6] K. Sinha, M. Barnhardt, and G.V. Candler. Detached eddy simulation of hypersonic base flows with application to Fire II experiments. AIAA Paper 2004-2633, 34th AIAA Fluid Dynamics Conference, 2004.

[7] C. C. Wong, F. G. Blottner, J. L. Payne, and M. Soetrisno. Implementation of a parallel algorithm for thermo-chemical nonequilibrium flow solutions. AIAA Paper 95-0152, January 1995.

[8] P. R. Spalart, W-H. Jou, M. Strelets, and S. R. Allmaras. Comments on the feasibility of LES for wings, and on a hybrid RANS/LES approach. Advances in DNS/LES, 1st AFOSR International Conference on DNS/LES, Greyden Press, 1997.

[9] J. H. Bell. Transonic/supersonic wind tunnel testing of the NASA Orion command module. AIAA 2007-1006, 2007.

Supplementary Material on the High-Order SLIP Scheme

A family of symmetric, characteristic-based flux difference schemes forms the starting point for construction of low-dissipation schemes. This type of scheme is termed Symmetric Total-Variation-Diminishing (STVD) by Yee and co-workers [3], and Symmetric Limited Positive (SLIP) by Jameson [2]. This choice of flux schemes is motivated by the fact that the numerical dissipation term in the scheme is explicitly separated from the non-dissipative, centered approximation to the flux, leading to a natural formulation for switched schemes that aim to reduce the numerical dissipation where it is not necessary.

Let $\mathbf{U}$ denote the conserved variables and $\mathbf{F}(\mathbf{U})$ denote the flux vector for the compressible Euler equations, so that

$$\frac{\partial \mathbf{U}}{\partial t} + \nabla \cdot \mathbf{F} = 0. \tag{3}$$

Consider a cell-centered finite volume method on a one-dimensional, uniform mesh with mesh points $j = 1, 2, \ldots, N$, and cell interfaces $j = 1/2, 3/2, \ldots, N + 1/2$. The first order Roe flux is

$$\mathbf{F}^{(1)}_{j+1/2} = \frac{1}{2}\left(\mathbf{F}_j + \mathbf{F}_{j+1}\right) - \frac{1}{2}\mathbf{R}_{j+1/2}\left|\mathbf{\Lambda}_{j+1/2}\right|\Delta\mathbf{v}_{j+1/2}, \tag{4}$$

where

$$\Delta\mathbf{v}_{j+1/2} = \mathbf{R}^{-1}_{j+1/2}\left(\mathbf{U}_{j+1} - \mathbf{U}_j\right) \tag{5}$$

is the characteristic variable vector at the $j + 1/2$ cell interface. The columns of $\mathbf{R}_{j+1/2}$ are the eigenvectors of the Roe flux Jacobian $\mathbf{A}_{j+1/2} \equiv \frac{\partial \mathbf{F}}{\partial \mathbf{U}}_{j+1/2}$, and $\mathbf{\Lambda}_{j+1/2}$ is the diagonal matrix containing the eigenvalues of $\mathbf{A}_{j+1/2}$.

A second order SLIP flux is constructed by adding to the first order flux an anti-dissipative term in the following manner.

$$\mathbf{F}^{SLIP2}_{j+1/2} = \mathbf{F}^{(1)}_{j+1/2} + \frac{1}{2}\mathbf{R}_{j+1/2}\left|\mathbf{\Lambda}_{j+1/2}\right| L(\Delta\mathbf{v}_{j-1/2}, \Delta\mathbf{v}_{j+1/2}, \Delta\mathbf{v}_{j+3/2}) \tag{6}$$

The limited average operator L ensures that the anti-dissipation is added only away from extrema in the solution, so that the scheme reverts to first order in the vicinity of an extremum. Such a scheme has "positive coefficients," ensuring stability in the L_∞ norm [2]. Further, a positive scheme is Local Extremum Diminishing (LED), which means that a local maximum (minimum) in the solution does not increase (decrease) in time for the semi-discrete problem. The LED property (alternatively called monotonicity) ensures that shock waves are captured without oscillations in the solution. The perspective of the present approach is that preservation of the LED property of a numerical flux scheme is desirable in the vicinity of the shock wave.

A fourth order accurate (on a uniform mesh) symmetric flux that does *not* lead to a positive scheme is

$$\begin{aligned}\mathbf{F}^{(4)}_{j+1/2} =& \frac{7}{12}\left(\mathbf{F}_j + \mathbf{F}_{j+1}\right) - \frac{1}{12}\left(\mathbf{F}_{j-1} + \mathbf{F}_{j+2}\right) - \frac{1}{2}\mathbf{R}_{j+1/2}|\mathbf{\Lambda}_{j+1/2}|\times \\ & \left(\Delta\mathbf{v}_{j+1/2} - \frac{2}{3}\left[\Delta\mathbf{v}_{j-1/2} + \Delta\mathbf{v}_{j+3/2}\right] + \frac{1}{6}\left[\Delta\mathbf{v}_{j-3/2} + \Delta\mathbf{v}_{j+5/2}\right]\right).\end{aligned} \tag{7}$$

This is the sum of a centered fourth order reconstruction and a fifth order linear dissipative term. Jameson [2] has generalized the construction of higher order SLIP schemes for a scalar equation by starting with a positive lower order scheme and adding to this scheme a corrective flux away from extrema. To recover the fourth order flux from the second order flux, the following corrective flux must be added:

$$\begin{aligned}\mathbf{F}^{C}_{j+1/2} = \mathbf{F}^{(4)}_{j+1/2} - \mathbf{F}^{SLIP2}_{j+1/2} = & \\ \frac{1}{12}\left(\left(\mathbf{F}_j - \mathbf{F}_{j-1}\right) - \left(\mathbf{F}_{j+2} - \mathbf{F}_{j+1}\right)\right) - \frac{1}{2}\mathbf{R}_{j+1/2}\left|\mathbf{\Lambda}_{j+1/2}\right| & \\ \left(-\frac{2}{3}\left(\Delta\mathbf{v}_{j-1/2} + \Delta\mathbf{v}_{j+3/2}\right) + \frac{1}{6}\left(\Delta\mathbf{v}_{j-3/2}\right) + L(\Delta\mathbf{v}_{j-1/2}, \Delta\mathbf{v}_{j+1/2}, \Delta\mathbf{v}_{j+3/2})\right) &\end{aligned} \tag{8}$$

To facilitate construction of the high-order correction for a system of equations, the characteristic decomposition is performed on the centered component of the corrective flux, giving

$$\begin{aligned}\mathbf{F}^C_{j+1/2} =& \frac{1}{12}\left(\mathbf{R}_{j-1/2}\mathbf{\Lambda}_{j-1/2}\Delta\mathbf{v}_{j-1/2} - \mathbf{R}_{j+3/2}\mathbf{\Lambda}_{j+3/2}\Delta\mathbf{v}_{j+3/2}\right) \\ & - \frac{1}{2}\mathbf{R}_{j+1/2}\left|\mathbf{\Lambda}_{j+1/2}\right|\left(-\frac{2}{3}\left(\Delta\mathbf{v}_{j-1/2} + \Delta\mathbf{v}_{j+3/2}\right) + \frac{1}{6}\right. \\ & \left.\left(\Delta\mathbf{v}_{j-3/2}\right) + L(\Delta\mathbf{v}_{j-1/2}, \Delta\mathbf{v}_{j+1/2}, \Delta\mathbf{v}_{j+3/2})\right)\end{aligned} \tag{9}$$

The eigenvector matrices $\mathbf{R}_{j-1/2}$, $\mathbf{R}_{j+3/2}$ are now approximated by the local matrix $\mathbf{R}_{j+1/2}$. This allows the correction to be written in terms of a single eigenvalue matrix times a sum of characteristic variables scaled by corresponding eigenvalues.

$$\begin{aligned}\mathbf{F}^C_{j+1/2} \approx& \mathbf{R}_{j+1/2}\left\{\frac{1}{12}\left(\mathbf{\Lambda}_{j-1/2}\Delta\mathbf{v}_{j-1/2} - \mathbf{\Lambda}_{j+3/2}\Delta\mathbf{v}_{j+3/2}\right)\right. \\ & - \frac{1}{2}\left|\mathbf{\Lambda}_{j+1/2}\right|\left(-\frac{2}{3}\left(\Delta\mathbf{v}_{j-1/2} + \Delta\mathbf{v}_{j+3/2}\right) + \frac{1}{6}\left(\Delta\mathbf{v}_{j-3/2}\right) + \right. \\ & \left.\left. L(\Delta\mathbf{v}_{j-1/2}, \Delta\mathbf{v}_{j+1/2}, \Delta\mathbf{v}_{j+3/2})\right)\right\} \\ \equiv& \mathbf{R}_{j+1/2}\mathbf{G}_{j+1/2}\end{aligned} \tag{10}$$

The difference between the exact fourth-order corrective flux in equation (9) and the approximate corrective flux in (10) is $O(\Delta x^2)$. This will result in a second order accurate scheme, but presumably one with lower error at a given Δx than the second order SLIP scheme.

A bound is now constructed that limits the higher order correction.

$$B^l_{j+1/2} = \left|\texttt{minmod}\left(\left|\Lambda_{j-1/2}\right|^{ll}\Delta v^l_{j-1/2}, \left|\Lambda_{j+1/2}\right|^{ll}\Delta v^l_{j+1/2}, \left|\Lambda_{j+3/2}\right|^{ll}\Delta v^l_{j+3/2}\right)\right| \tag{11}$$

The superscript l refers to the particular element of a vector, while the double superscript refers to an element of a matrix. The corrective flux is added to the second order flux as long as its absolute value does not exceed the bound, giving the "fourth order" SLIP flux

$$\mathbf{F}^{SLIP4}_{j+1/2} = \mathbf{F}^{SLIP2}_{j+1/2} + \mathbf{R}_{j+1/2}\mathbf{\Psi}_{j+1/2}, \tag{12}$$

where

$$\Psi^l_{j+1/2} = \text{sign}\left(G^l_{j+1/2}\right)\min\left(\left|G^l_{j+1/2}\right|, B^l_{j+1/2}\right). \tag{13}$$

It is proven in Ref. [2] that, for a scalar conservation equation, if the lower order scheme is LED, then, using the above construction, the higher order SLIP scheme will also be LED.

Ensuring Higher Order at a Smooth Extremum

In construction of the fourth order SLIP scheme, recall that the high-order correction term was only added when it was less than some bound $B_{j+1/2}$ (see Equation (11)). Suppose now that the wavelet sensor detects smooth flow and so the dissipative term $\mathbf{\Phi}^{(4)}_{j+1/2}$ in the

corrective flux is zero. But the correction to the centered difference component of the scheme is still contained in the corrective flux. If the face $j+1/2$ is an extremum of a characteristic variable, then the bound will be zero and no corrective flux will be added. Since the function is smooth, accuracy will be increased if the corrective flux is added. A way to ensure this is to replace the bound $B^l_{j+1/2}$ from Equation (11) with

$$B^l_{j+1/2} = \max\left(B^l_{j+1/2}, \quad (1-\theta^l_{j+1/2})\min(|\Delta v^l_{j-1/2}|, |\Delta v^l_{j+1/2}|, |\Delta v^l_{j+3/2}|)\right) \tag{14}$$

When $\theta^l_{j+1/2} = 1$ in a non-smooth region, the high-order correction will remain bounded by $B^l_{j+1/2}$, which is going to be zero at an extremum due to the action of the `minmod` operator. However, if $\theta^l_{j+1/2} < 1$, implying some smoothness in the solution, some correction can still be added, even at an extremum. The bound on the correction is arbitrarily chosen to vary linearly with the value of the flow sensor. The scheme thus remains LED whenever the wavelet sensor detects a discontinuity, but is no longer LED when the wavelet sensor detects smooth flow.